Molecular & Biochemical Parasitology 223 (2018) 50–54

Contents lists available at ScienceDirect

Molecular & Biochemical Parasitology

journal homepage: www.elsevier.com/locate/molbiopara

Recombinant and native *Tvi*CATL from *Trypanosoma vivax*: Enzymatic characterisation and evaluation as a diagnostic target for animal African trypanosomosis

Lauren E.-A. Eyssen[a], Perina Vather[a], Laurelle Jackson[a], Phindile Ximba[a], Nicolas Biteau[b], Théo Baltz[b], Alain Boulangé[a,c,d,e], Philippe Büscher[f], Theresa H.T. Coetzer[a,*]

[a] Biochemistry, School of Life Sciences, University of KwaZulu-Natal (Pietermaritzburg campus), Private Bag X01, Scottsville, 3209, South Africa
[b] Laboratoire de Microbiologie Fondamentale et Pathogénicité, Université Bordeaux. UMR-CNRS 5234, 146, Rue Léo Saignat, 33076, Bordeaux Cedex, France
[c] CIRAD, UMR INTERTRYP, 01009 Maputo, Mozambique
[d] INTERTRYP, Univ Montpellier, CIRAD, IRD, Montpellier, France
[e] Centro de Biotecnologia, Universidade Eduardo Mondlane, 01009 Maputo, Mozambique
[f] Department of Biomedical Sciences, Institute of Tropical Medicine, Nationalestraat 155, B-2000, Antwerp, Belgium

ARTICLE INFO

Keywords:
Trypanosoma vivax
Nagana
Cathepsin L-like peptidase
*Tvi*CATL
Diagnostic target

ABSTRACT

African animal trypanosomosis (*nagana*) is caused by tsetse-transmitted protozoan parasites. Their cysteine proteases are potential chemotherapeutic and diagnostic targets. The *N*-glycosylated catalytic domain of *Trypanosoma vivax* cathepsin L-like cysteine protease, r*Tvi*CATL$_{cat}$, was recombinantly expressed and purified from culture supernatants while native *Tvi*CATL was purified from *T. vivax* Y486 parasite lysates. Typical of Clan CA, family C_1 proteases, *Tvi*CATL activity is sensitive to E-64 and cystatin and substrate specificity is defined by the S_2 pocket. Leucine was preferred in P_2 and basic and non-bulky, hydrophobic residues accepted in P_1 and P_3 respectively. Reversible aldehyde inhibitors, antipain, chymostatin and leupeptin, with Arg in P_1 and irreversible peptidyl chloromethylketone inhibitors with hydrophobic residues in P_2 inhibited *Tvi*CATL activity. *Tvi*CATL digested host proteins: bovine haemoglobin, serum albumin, fibrinogen and denatured collagen (gelatine) over a wide pH range, including neutral to slightly acidic pH. The recombinant catalytic domain of *Tvi*CATL showed promise as a diagnostic target for detecting *T. vivax* infection in cattle in an indirect antibody detection ELISA.

Tsetse (*Glossina* spp) -transmitted haemoprotozoan parasites of the genus *Trypanosoma* (order *Kinetoplastidae*), *T.* (*Nanomonas*) *congolense, T.* (*Dutonella*) *vivax,* and to a lesser extent, *T.* (*Trypanozoon*) *brucei brucei,* cause animal African trypanosomosis (AAT) in livestock, most importantly cattle, in sub-Saharan Africa. Infected wild animals remain asymptomatic and are trypanosome reservoirs [1]. The disease is also known as *nagana* from the Zulu word "*unakane*" that means continual pestering action, referring to tsetse flies and by extension to the resulting disease in cattle (Andrew Koopman, Emeritus Professor of isiZulu Studies, University of KwaZulu-Natal, personal communication). Contrary to *T. congolense,* which develops in the midgut of the tsetse fly, *T. vivax* is confined to the vector mouthparts. Consequently, *T. vivax* is also spread by biting flies (*Tabanus* and *Stomoxys* spp), allowing establishment in Central and South America where it is now widespread among cattle with 25–50% sero-prevalence [2]. *Nagana* is a wasting disease that is either acute, killing animals within a month, or, most commonly, chronic, lasting for several years. The disease manifests as intermittent fever, anaemia, general weakness and loss of condition, lymphadenopathy, abortion, and lacrimation, resulting in high levels of morbidity, mortality, and infertility in livestock. This impacts on the livelihood of resource-poor rural farmers and costs the African continent billions of US$ annually [3].

Trypanosomes evade the mammalian host immune system by cyclically switching the expression of their variable surface glycoproteins (VSG). This makes the development of a classical vaccine unlikely. Currently available animal trypanocides have been in use for over 60 years resulting in increasing incidences of drug resistance [4]. There is thus a critical need to identify new drug targets and since effective chemotherapy requires accurate diagnosis, identifying and testing new diagnostic targets are ongoing [5,6].

Parasite cathepsin L- and B-like cysteine peptidases (proteases or proteolytic enzymes) are released into the host bloodstream upon

* Corresponding author.
E-mail address: coetzer@ukzn.ac.za (T.H.T. Coetzer).

https://doi.org/10.1016/j.molbiopara.2018.07.001
Received 10 April 2018; Received in revised form 29 June 2018; Accepted 4 July 2018
Available online 07 July 2018
0166-6851/ © 2018 Elsevier B.V. All rights reserved.

parasite lysis and have been implicated in the pathogenesis associated with *T. congolense*, *T. b. brucei*, *T. cruzi* and *Leishmania* spp. infections [7–9]. Although there are endogenous cysteine protease inhibitors such as the kininogens and cystatin C in the host blood stream, unusual active complexes have been reported between parasite or host cysteine proteases and kininogens that may contribute to pathology [7]. Consequently, parasite cysteine peptidases were identified as targets for the development of chemotherapies and diagnostics [5].

Congopain or *Tco*CATL (nomenclature proposed by [10]) and *Tvi*CATL, the major cathepsin L-like peptidase in *T. congolense* and *T. vivax* respectively, are expressed in the mammalian infective bloodstream form parasites [8,11]. The genes coding for both *Tco*CATL and *Tvi*CATL-like peptidases comprise a multigene family organized as a tandem array. Several of the *Tco*CATL genes display substitutions in the active site residues Cys^{25}, His^{191}, Asn^{211} (*Tco*CATL numbering) where Ser replaces Cys^{25} and less frequently Ser or Tyr replaces His^{191} [8]. CATL peptidases typically consist of a signal peptide, pro-peptide and catalytic domain. The active peptidase results from low pH removal of the pro-peptide that, in the case of *Tco*CATL and *Tcr*CATL, contain an inhibitory YHNGA (YHNGE in *Tvi*CATL; Supplementary Fig. S1) motif [7]. Kinetoplast CATL peptidases, unlike their mammalian homologues, also contain a highly immunogenic 11–13 kDa C-terminal extension of unknown function [7,10]. The multigene family coding for *Tvi*CATL has been identified and shown to be good molecular diagnostic targets for epidemiological studies [11], but the expressed peptidase has not been characterised to date.

Here we compare the enzymatic characteristics of the native form of the enzyme isolated from *T. vivax* Y486 parasites (n*Tvi*CATL*)* and the purified recombinant catalytic domain (r*Tvi*$CATL_{cat}$). Recombinant *Tvi*$CATL_{cat}$ was also evaluated as a diagnostic antigen to discriminate between infected and non-infected cattle by testing a blinded panel of sera from cattle, experimentally infected with *T. vivax*, in an indirect antibody detection ELISA format.

Recombinant expression in *Pichia pastoris* and purification using three phase partitioning, molecular exclusion and anion exchange chromatography (Supplementary Table S1) yielded r*Tvi*$CATL_{cat}$ of 28 and 32 kDa (catalytic domain only, confirmed by amino acid sequencing, result not shown), while a 44 kDa native form, n*Tvi*CATL, containing the intact C-terminal extension, was purified from *T. vivax* (Y486) lysates (Fig. 1A, lanes 1 and 3). The native and recombinant forms of *Tvi*CATL could be distinguished using affinity purified chicken anti-*Tvi*CATL C-terminal extension peptide (TAPGPSSTKTLCSGDDC) IgY and bovine anti-*Tco*CATL catalytic domain IgG in western blots (Fig. 1A, lanes 2 and 4).

*Tvi*CATL is predicted to be *N*-glycosylated at Asn^{288} (*Tvi*CATL numbering; Supplementary Fig. S1; Prosite P000001 (http://prosite.expasy.org/scanprosite/)) possibly accounting for the two bands observed in Fig. 1A, lane 1. Incubation of r*Tvi*$CATL_{cat}$ with endoglycosidase H, decreased the size of the 32 kDa band to a single 28 kDa band (Fig. 1B) confirming the *N*-glycosylated nature of r*Tvi*$CATL_{cat}$. Glycosylation was similarly demonstrated for *Tcr*CATL2 [12] and *Tbr*CATL [13], predicted to be glycosylated in the equivalent positions (Asn^{292} and Asn^{295} respectively, Supplementary Fig. S1). By comparison, *Tco*CATL is not glycosylated [14] and has an Asn^{288}Asp substitution in this position (Supplementary Fig. S1). Both glycosylated 32 kDa- and non-glycosylated 28 kDa r*Tvi*$CATL_{cat}$ were recognised by antibodies produced against the catalytic domain of *Tco*CATL (Fig. 1A, lane 2) as a result of the high level of sequence identity of 70% between the catalytic domains of the homologues (Supplementary Fig. S1).

Knowledge of the substrate specificity of trypanosomal proteases is essential for the development of inhibitors with anti-trypanosomal potential. The substrate specificity of r*Tvi*$CATL_{cat}$ and n*Tvi*CATL was assessed with a range of fluorogenic peptide substrates that differed in their amino acid residues at P_1, P_2 and P_3 which bind to S_1, S_2 and S_3 in the active site cleft respectively (Fig. 1C; Supplementary Table S2). For r*Tvi*$CATL_{cat}$, H-D-Val-Leu-Lys-7-amido-4-methylcoumarin (AMC) was the best substrate (k_{cat}/K_m 38.61 $s^{-1}\,mM^{-1}$) followed by Z-Phe-Arg-AMC (k_{cat}/K_m 22.57 $s^{-1}\,mM^{-1}$). For n*Tvi*CATL, H-D-Ala-Leu-Lys-AMC was a slightly better substrate than H-D-Val-Leu-Lys-AMC, (k_{cat}/K_m of 72.42 $s^{-1}.\,mM^{-1}$ vs 60.19 $s^{-1}\,mM^{-1}$). Both r*Tvi*$CATL_{cat}$ and n*Tvi*CATL thus prefer basic amino acids, Lys and Arg, in the P_1 position and large hydrophobic amino acids, Phe or Leu, in P_2 and tolerate a variety of residues in P_3. Both *Tcr*CATL and *Tbr*CATL preferred Leu over Phe in P_2 in a diversified positional scanning synthetic combinatorial library [15]. Also preferring Leu and Lys at the P_2 and P_1 positions respectively, is the catalytic domain of recombinant *Tco*CATL and native *Tco*CATL [8]. The inability of both r*Tvi*$CATL_{cat}$ and n*Tvi*CATL to hydrolyse Z-Arg-Arg-AMC demonstrates a lack of CATB-like character. Hydrolysis of Z-Pro-Arg-AMC by r*Tvi*$CATL_{cat}$ corresponds to the marked preference of mammalian cathepsin K for Pro at P_2 [15]. This hydrolytic specificity is consistent with the presence of a Leu at the bottom of the S_2 subsite of both *Tvi*CATL and cathepsin K. Hydrolysis of a proline containing peptide substrate is consistent with the finding that *Tvi*CATL is able to hydrolyse proline-rich gelatin (Fig. 2E).

Although the yeast-expressed r*Tvi*$CATL_{cat}$ comprises a mixture of glycosylated and non-glycosylated peptidase, these results suggest that glycosylation does not affect the catalytic specificity. From the data in Fig. 1C, it is evident that both r*Tvi*$CATL_{cat}$ and n*Tvi*CATL have a substrate specificity defined by the S_2 position, which is consistent with the properties of the cysteine proteases, clan CA, family C1, to which *Tvi*CATL belongs.

The rate of hydrolysis of H-D-Val-Leu-Lys-AMC, the substrate with the highest k_{cat}/K_m for r*Tvi*$CATL_{cat}$ (Fig. 1C), was tested in constant ionic strength Acetate-MES-Tris buffers over a range of pH values to determine the pH optimum of purified r*Tvi*$CATL_{cat}$ and n*Tvi*CATL (Fig. 1D). Although r*Tvi*$CATL_{cat}$ functions optimally over a slightly narrower pH range than n*Tvi*CATL, similar pH optima of 7.0 (r*Tvi*$CATL_{cat}$) and 7.5 (n*Tvi*CATL) were obtained, suggesting that *Tvi*CATL is active in the host bloodstream following parasite lysis. Although *Tbr*CATL and *Tcr*CATL [13] have acidic pH optima (5.0–5.5), these homologues also showed considerable peptidase activity and stability remaining at neutral pH. The only variation between the pH activity profiles for full-length n*Tvi*CATL and truncated r*Tvi*$CATL_{cat}$ was retention of some activity at acidic pH for the native form (60% at pH 5.5 and 40% at pH 5.0). The C-terminal extension of n*Tvi*CATL is unlikely to influence the activity at acidic pH since full length and truncated *Tbr*CATL have very similar pH profiles [13]. Retention of activity at acidic pH by the native form is consistent with the lysosomal localisation of these peptidases.

The cysteine peptidase inhibitor, cystatin, was the most effective inhibitor of H-D-Val-Leu-Lys-AMC hydrolysis by both n*Tvi*CATL and r*Tvi*$CATL_{cat}$ with *K*i values of 0.5 and 1.41 mM respectively (Table 1). Peptidyl-diazomethyl ketone inhibitors based on the conserved structures of cystatin C, Z-RLVG-CHN_2, inhibit native *Tco*CATL and *Tcr*CATL [7,16] and would in all likelihood be effective inhibitors of *Tvi*CATL. Both n*Tvi*CATL and r*Tvi*$CATL_{cat}$ were inhibited by leupeptin, chymostatin and antipain. While there was little discrimination among the inhibition of H-D-Ala-Leu-Lys-AMC and Z-Phe-Arg-AMC hydrolysis by r*Tvi*$CATL_{cat}$, some discrimination was observed for the inhibition of H-D-Val-Leu-Lys-AMC hydrolysis by these inhibitors. No inhibition by bestatin, EDTA and pepstatin A confirmed that *Tvi*CATL is neither a metal ion dependent- nor an aspartic peptidase.

Both r*Tvi*$CATL_{cat}$ and n*Tvi*CATL were inhibited by the irreversible Gly-Leu-Phe-CH_2Cl and H-D-Val-Phe-Lys-CH_2Cl peptidyl chloromethylketone inhibitors (Table 1). Consistent with the preference for Leu over Phe in the P_2 position, the former was the marginally better inhibitor. Consequently, the peptidyl vinyl sulfone, K11017 with a homophenylalanine at P_1 and Leu at P_2 that inhibits falcipain-3 (cysteine peptidase from *Plasmodium falciparum*; *Pfa*CATL3), *Tcr*CATL and *Tbr*CATL [17], has potential to inhibit *Tvi*CATL. The alkylating thiol group inhibitors, iodoacetamide and iodoacetate, inhibited *Tvi*CATL but not as effectively as the chloromethylketone inhibitors. No inhibition

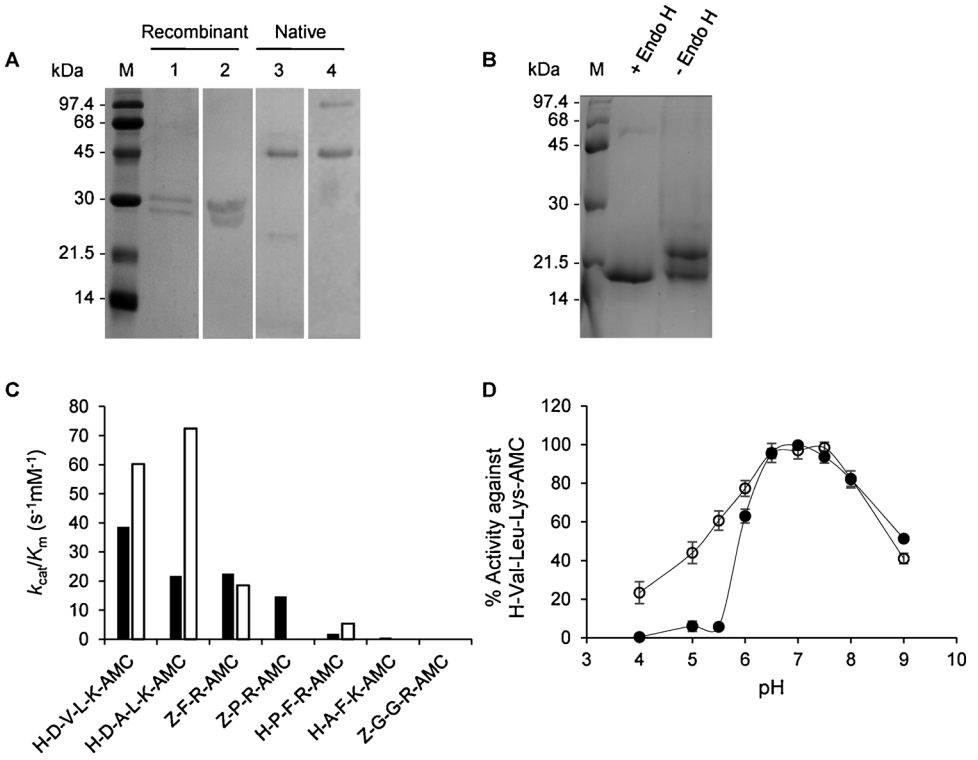

Fig. 1. Characterisation of purified r*Tvi*CATL$_{cat}$ and n*Tvi*CATL. (A) Reducing SDS-PAGE and western blot of samples from expressed and purified r*Tvi*CATL$_{cat}$ (lane 1) and n*Tvi*CATL (lane 3) were separated on a 12.5% reducing SDS-PAGE gel and either silver stained (lanes 1 and 3) or transferred onto nitrocellulose and r*Tvi*CATL$_{cat}$ was probed with bovine anti-catalytic domain of *Tco*CATL IgY (lane 2) and n*Tvi*CATL with affinity purified chicken anti-C-terminal extension peptide (TAPGPSSTKTLCSGDDC) IgY (lane 4). The blot was developed using 4-chloro-1-naphthol-H_2O_2. (B) Analysis of the deglycosylation of r*Tvi*CATL$_{cat}$. Purified r*Tvi*CATL$_{cat}$ samples, incubated in the presence of (+) or absence of (−) endoglycosidase H, were electrophoresed on a 12.5% reducing SDSPAGE gel and stained with Coomassie blue R-250. Lane M, molecular mass markers. (C) Substrate specificity was established by pre-incubation of r*Tvi*CATL$_{cat}$ (■) or n*Tvi*CATL (□), using 1.5 ng active enzyme (determined by E64 titration) in assay buffer (100 mM Bis-Tris buffer, pH 6.5, 4 mM Na_2EDTA, 0.02% (w/v) NaN_3, 8 mM DTT) for 5 min at 37 °C before various fluorogenic peptide substrates (20 μM) were added. The initial steady-state velocity (v_0) was determined by continuous assay for a range of substrate concentrations (2.5 to 50 μM). K_m and V_{max} were determined by hyberbolic regression of the kinetic data. The k_{cat} was determined from $k_{cat} = V_{max}/[E]_0$, where $[E]_0$ represents the active enzyme concentrations (Supplementary Table S2). D. Optimum pH for substrate hydrolysis by r*Tvi*CATL$_{cat}$ and n*Tvi*CATL. The enzymatic activity of *Tvi*CATL was measured using constant ionic strength AMT buffers (100 mM acetic acid, 200 mM TrisHCl, 100 mM MES, 8 mM DTT, 4 mM EDTA) in a pH range of 4.0 to 9.0. Active enzyme (1.5 ng, determined by E64 titration) was incubated at 37 °C for 15 min with the buffers at different pH-values. The hydrolysis of H-D-Val-Leu-Lys-AMC, performed in triplicate, by r*Tvi*CATL$_{cat}$ (●) and n*Tvi*CATL (○) was measured (Ex_{360}; Em_{460}).

was noted for typical serine peptidase inhibitors, PMSF, TLCK and TPCK.

To evaluate whether *Tvi*CATL could potentially be involved in trypanosome pathogenesis through degradation of host proteins and tissues, r*Tvi*CATL$_{cat}$ was incubated with different protein substrates in a pH range of 5–9 (Fig. 2A–D). Bovine haemoglobin (67 kDa) was partially hydrolysed over the pH range of 5–9 (Panel A) shown by the reduction in intensity of the 15 kDa α- and β-monomers and the 30 kDa αβ dimers when compared to the sample without peptidase. Bovine serum albumin was completely hydrolysed at pH 5 and 5.5, partially at pH 6–7.5 and not hydrolysed at pH 8 and 9 (Panel B). Over the pH-range of 5–7.5 the α (63.5 kDa), β- (56 kDa) and γ- (47 kDa) chains of bovine fibrinogen [18] were readily hydrolysed by r*Tvi*CATL$_{cat}$ as seen by a decrease in intensity of the protein bands (Panel C). By comparison, n*Tvi*CATL was able to digest the 63.5 kDa α and 56 kDa βchains of fibrinogen, but not the 47 kDa γ-chain during a one-hour incubation time (Panel D). Incubation of the respective protein substrates at the different pH-values for 16 h without r*Tvi*CATL$_{cat}$ had no effect (Supplementary Fig. S2). This observation that *Tvi*CATL is able to degrade host proteins at a physiological pH gives further support for the possible involvement of *Tvi*CATL in pathogenesis.

Gelatinase activity of r*Tvi*CATL$_{cat}$ was observed between 30 and 45 kDa on a gelatin-containing zymogram (Fig. 2E, "no inhibitor" lane; approximate sizes for a non-reducing gelatin SDS-PAGE gel). However, only after an extended incubation period of 9 h, was hydrolysis by n*Tvi*CATL observed at approximately 68 kDa (result not shown). Compared to where no inhibitor was added, the specific cysteine protease inhibitor, E-64, as well as the cysteine/serine protease inhibitors, antipain, leupeptin and iodoacetate, completely inhibited the gelatinase activity of r*Tvi*CATL$_{cat}$ (Fig. 2E). The irreversible cysteine protease inhibitors, Z-Gly-Leu-Phe-CH_2Cl, chymostatin and stefin B partially inhibited the activity of r*Tvi*CATL$_{cat}$, whilst bestatin and EDTA did not show any inhibition. These results correlate well with the data in Table 1 and provide further evidence that *Tvi*CATL is a cysteine peptidase.

The diagnostic potential of the r*Tvi*CATL$_{cat}$ antigen was tested in an indirect antibody detection ELISA format using a blinded panel of sera from non-infected and cattle experimentally infected with *T. vivax* (Supplementary Table S3). An Area Under the Curve (AUC) value of 0.78 (95% CI 0.672–0.88) with a p value of < 0.0001 demonstrates that the r*Tvi*CATL$_{cat}$ antigen was able to discriminate between serum from infected and noninfected cattle (Supplementary Fig. S3). At the highest Youden index (0.588), found at a cut-off value of 0.0563, the sensitivity was 71.9% and the specificity 86.0% (Supplementary Table S4). A higher sensitivity combined with lower specificity was reported in another antibody detection ELISA using crude parasite lysates as antigen [19]. Further evaluation of the diagnostic potential of the r*Tvi*CATL$_{cat}$ antigen should include testing sera from cattle naturally infected with *T. vivax* and adapting the test to a lateral flow format (rapid diagnostic test or RDT), as was done for the recently developed RDT prototypes based on an invariant surface glycoprotein [6] and *Tvi*GM6, a tandem repeat flagellar protein for *T. vivax* and *Tco*CATB for *T. congolense* [5], that show much promise. Since specific antibodies persist for several weeks after cure, the ideal diagnostic test would rather be an antigen capture ELISA or RDT, which is able to detect circulating parasite antigen(s), indicative of an active infection, rather than antibodies. However, little progress has been made in identifying a suitable trypanosome antigen and producing the corresponding antibodies for a sandwich ELISA [20].

Taken together, our data showed that the *T. vivax* cathepsin L-like peptidase, *Tvi*CATL, has a pronounced preference for hydrophobic residues Phe or Leu at the P_2 position, and that the activity of *Tvi*CATL is inhibited by class-specific cysteine peptidase inhibitors. At a physiological pH, *Tvi*CATL was able to hydrolyse a number of protein substrates

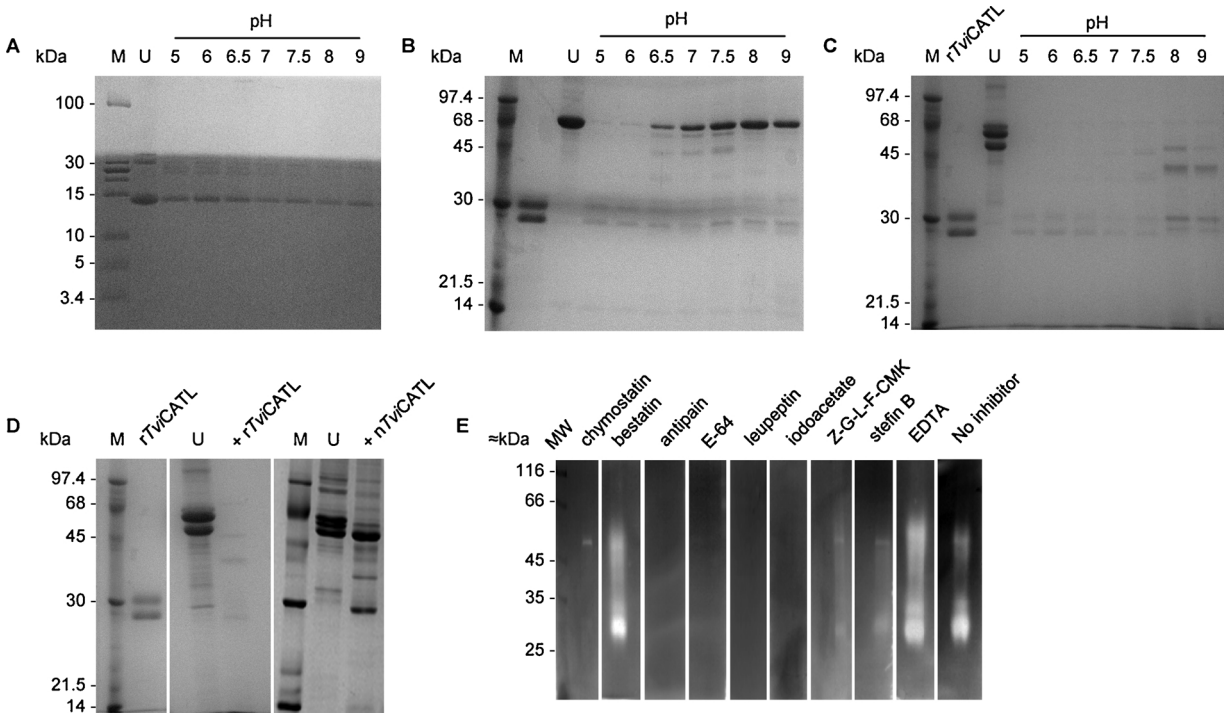

Fig. 2. Hydrolysis of protein substrates by *Tvi*CATL. Recombinant *Tvi*CATL (1 μg E-64 titrated active enzyme) was combined with 1 mg/ml of each of bovine haemoglobin, bovine serum albumin (BSA), or bovine fibrinogen in 50 mM citrate, 100 mM sodium phosphate buffer containing 2 mM dithiothreitol (DTT) over a pH range of 5–9 and incubated for 16 h at 37 °C. The reaction was stopped by addition of reducing treatment buffer followed by boiling at 100 °C for 2 min. Reducing SDS-PAGE analysis of r*Tvi*CATL hydrolysis of (A) haemoglobin on a 16% T/6% C, 6 M Urea Tris-Tricine gel, (B) BSA on a 15% and (C) fibrinogen on a 12.5% Tris-Glycine gel. (D) Comparative hydrolysis of fibrinogen (8.8 μM) by r*Tvi*CATL$_{cat}$ or n*Tvi*CATL (0.088 μM active enzyme) in 100 mM Tris–HCl buffer, 30 mM cysteine, pH 7.4 for 1 h at 37 °C. Proteolysis was stopped by the addition of 1 mM E64 and samples analysed by 12.5% reducing SDS-PAGE and stained with Coomassie blue R 250. Untreated protein substrates (U) were loaded to assist in the visualization of hydrolysis by *Tvi*CATL. (E) Gelatinase activity of r*Tvi*CATL$_{cat}$ in the presence of inhibitors. Samples of r*Tvi*CATL$_{cat}$ (1 μg, active enzyme by E-64 titration) was separated on a 1% gelatin-containing non-reducing 12.5% SDS-PAGE gel. After the electrophoresis and detergent exchange, the gel was cut into strips and each was incubated in assay buffer (100 mM Bis-Tris buffer, pH 6.5, 4 mM Na_2EDTA, 0.02% (w/v) NaN_3, 8 mM DTT) supplemented with their respective inhibitor [chymostatin (10 μM), bestatin (10 μM), antipain (10 μM), E-64 (10 μM), leupeptin (10 μM), iodoacetate (10 μM), Z-Gly-Leu-Phe- CH_2Cl (50 μM), stefin B (80 μM) or EDTA (10 mM), final concentrations] at 37 °C for 16 h before staining with Amido black. Note that kDa values of the molecular weight markers are approximate under non-reducing conditions.

suggesting that it might be active in the bloodstream following parasite lysis. The indirect antibody detection ELISA based on the r*Tvi*CATL$_{cat}$ antigen was able to discriminate between serum from non-infected and *T. vivax*-infected cattle.

Acknowledgements

The work was supported by grants from the 5th and 6th Framework programme of the European Commission priority INCO-DEV, projects Trypadvac and Trypadvac2, contracts ICA4-CT-2000-30035 and PL003716, the National Research Foundation of South Africa (grant

Table 1
Irreversible and reversible inhibitors of r*Tvi*CATL$_{cat}$ and n*Tvi*CATL.

Irreversible Inhibitors	Recombinant						Native	
	Z-Phe-Arg-AMC		H-D-Ala-Leu-Lys-AMC		H-D-Val-Leu-Lys-AMC			
	k_{ass}[a] ($mM^{-1}\,s^{-1}$)	$t_{1/2}$ (s)	k_{ass} ($mM^{-1}\,s^{-1}$)	$t_{1/2}$ (s)	k_{ass} ($mM^{-1}\,s^{-1}$)	$t_{1/2}$ (s)	k_{ass} ($mM^{-1}\,s^{-1}$)	$t_{1/2}$ (s)
Z-Gly-Leu-Phe-CH_2Cl	28.57 ± 0.02	798	7.1 ± 0.01	3192	107.00 ± 6.51	213	89.50 ± 11.21	254
H-D-Val-Phe-Lys-CH_2Cl	ND	ND	ND	ND	85.08 ± 4	ND	74.02 ± 6.23	ND
Iodoacetic acid	71.4 ± 0.025	319	71.4 ± 0.025	319	17.86 ± 5.04	1386	31.50 ± 1.01	724
Iodoacetamide	35.70 ± 0.01	638	35.1 ± 0.025	639	12.50 ± 7.58	1980	35.00 ± 2.76	652

Reversible inhibitors	*Ki* (mM) (x 10^3)	*Ki* (mM) (x 10^3)	*Ki* (mM) (x 10^3)	*Ki* (mM) (x 10^3)
Cystatin	ND[b]	ND	1.41	0.5
Leupeptin	4.46	1.8	4.35	1.24
Chymostatin	9.77	1.18	18.07	4.5
Antipain	13.32	1.14	11.4	15.05

[a] k_{ass} ± SD (n = 3); No inhibition was detected with Boc-Val-Leu-Gly-Lys-CHN_2, PMSF, phenylmethanesulfonyl fluoride; TLCK, Nα-Tosyl-Lys-chloromethyl ketone and TPCK, L-1-tosylamido-2-phenylethyl chloromethyl ketone.

[b] ND: Not determined experimentally. No inhibition was detected with EDTA (10 mM), bestatin (10 μM), pepstatin A (1 μM).

CSUR14080586633) and the Global Alliance for Livestock Veterinary Medicines (GALVmed). We would like to thank Grant Napier (formerly GALVmed), Josephus Fourie, Heidi Erasmus and Annesca Joubert (ClinVet) for providing sera and facilities to conduct ELISAs.

Appendix A. Supplementary data

Supplementary data associated with this article can be found, in the online version, at https://doi.org/10.1016/j.molbiopara.2018.07.001.

References

[1] C.J. de Beer, G.J. Venter, K. Kappmeier Green, J. Esterhuizen, D.G. de Klerk, J. Ntshangase, M.J. Vreysen, R. Pienaar, M. Motloang, L. Ntantiso, A.A. Latif, An update of the tsetse fly (Diptera: *Glossinidae*) distribution and African animal trypanosomosis prevalence in north-eastern KwaZulu-Natal, South Africa, Onderstepoort J. Vet. Res. 83 (1) (2016) a1172.

[2] M.I. Gonzatti, B. González-Baradat, P.M. Aso, A. Reyna-Bello, *Trypanosoma* (*Duttonella*) *vivax* and typanosomosis in Latin America: Secadera/Huequera/Cacho Hueco, in: S. Magez, M. Radwanska (Eds.), Trypanosomes and Trypanosomiasis, Springer-Verlag, Vienna, 2014.

[3] A.P. Shaw, G.R. Wint, G. Cecchi, S.J. Torr, R.C. Mattioli, T.P. Robinson, Mapping the benefit-cost ratios of interventions against bovine trypanosomosis in Eastern Africa, Prev. Vet. Med. 122 (4) (2015) 406–416.

[4] F. Giordani, L.J. Morrison, T.G. Rowan, D.E.K. HP, M.P. Barrett, The animal trypanosomiases and their chemotherapy: a review, Parasitology 143 (14) (2016) 1862–1889.

[5] A. Boulangé, D. Pillay, C. Chevtzoff, N. Biteau, V. Come de Graca, L. Rempeters, D. Theodoridis, T. Baltz, Development of a rapid antibody test for point-of-care diagnosis of animal African trypanosomosis, Vet. Parasitol. 233 (2017) 32–38.

[6] J.R. Fleming, L. Sastry, S.J. Wall, L. Sullivan, M.A. Ferguson, Proteomic identification of immunodiagnostic antigens for *Trypanosoma vivax* infections in cattle and generation of a proof-of-concept lateral flow test diagnostic device, PLoS Negl. Trop. Dis. 10 (9) (2016) e0004977.

[7] G. Lalmanach, A. Boulangé, C. Serveau, F. Lecaille, J. Scharfstein, F. Gauthier, E. Authié, Congopain from *Trypanosoma congolense*: drug target and vaccine candidate, Biol. Chem. 383 (5) (2002) 739–749.

[8] D. Pillay, A.F. Boulangé, T.H. Coetzer, Expression, purification and characterisation of two variant cysteine peptidases from *Trypanosoma congolense* with active site substitutions, Protein Expr. Purif. 74 (2) (2010) 264–271.

[9] C. Mendoza-Palomares, N. Biteau, C. Giroud, V. Coustou, T. Coetzer, E. Authié, A. Boulangé, T. Baltz, Molecular and biochemical characterization of a cathepsin B-like protease family unique to *Trypanosoma congolense*, Eukaryot. Cell 7 (4) (2008) 684–697.

[10] C.R. Caffrey, D. Steverding, Kinetoplastid papain-like cysteine peptidases, Mol. Biochem. Parasitol. 167 (1) (2009) 12–19.

[11] A.P. Cortez, A.C. Rodrigues, H.A. Garcia, L. Neves, J.S. Batista, Z. Bengaly, F. Paiva, M.M. Teixeira, Cathepsin L-like genes of *Trypanosoma vivax* from Africa and South America-characterization, relationships and diagnostic implications, Mol. Cell. Probes 23 (1) (2009) 44–51.

[12] A.E. Eakin, M.E. McGrath, J.H. McKerrow, R.J. Fletterick, C.S. Craik, Production of crystallizable cruzain, the major cysteine protease from *Trypanosoma cruzi*, J. Biol. Chem. 268 (9) (1993) 6115–6118.

[13] C.R. Caffrey, E. Hansell, K.D. Lucas, L.S. Brinen, A. Alvarez Hernandez, J. Cheng, S.L. Gwaltney 2nd, W.R. Roush, Y.D. Stierhof, M. Bogyo, D. Steverding, J.H. McKerrow, Active site mapping, biochemical properties and subcellular localization of rhodesain, the major cysteine protease of *Trypanosoma brucei rhodesiense*, Mol. Biochem. Parasitol. 118 (1) (2001) 61–73.

[14] A.F. Boulangé, S.A. Khamadi, D. Pillay, T.H. Coetzer, E. Authié, Production of congopain, the major cysteine protease of *Trypanosoma* (*Nannomonas*) *congolense*, in *Pichia pastoris* reveals unexpected dimerisation at physiological pH, Protein Expr. Purif. 75 (1) (2011) 95–103.

[15] Y. Choe, F. Leonetti, D.C. Greenbaum, F. Lecaille, M. Bogyo, D. Bromme, J.A. Ellman, C.S. Craik, Substrate profiling of cysteine proteases using a combinatorial peptide library identifies functionally unique specificities, J. Biol. Chem. 281 (18) (2006) 12824–12832.

[16] J.R. Chagas, E. Authié, C. Serveau, G. Lalmanach, L. Juliano, F. Gauthier, A comparison of the enzymatic properties of the major cysteine proteinases from *Trypanosoma congolense* and *Trypanosoma cruzi*, Mol. Biochem. Parasitol. 88 (1–2) (1997) 85–94.

[17] I.D. Kerr, J.H. Lee, C.J. Farady, R. Marion, M. Rickert, M. Sajid, K.C. Pandey, C.R. Caffrey, J. Legac, E. Hansell, J.H. McKerrow, C.S. Craik, P.J. Rosenthal, L.S. Brinen, Vinyl sulfones as antiparasitic agents and a structural basis for drug design, J. Biol. Chem. 284 (38) (2009) 25697–25703.

[18] R. Gollwitzer, R. Timpl, U. Becker, H. Furthmayr, Chemical and immunological properties of reduced and alkylated polypeptide chains of bovine fibrinogen, Eur. J. Biochem. 28 (4) (1972) 497–506.

[19] J.W. Magona, J.S. Mayende, J. Walubengo, Comparative evaluation of the antibody-detection ELISA technique using microplates precoated with denatured crude antigens from Trypanosoma congolense or Trypanosoma vivax, Trop. Anim. Health Prod. 34 (4) (2002) 295–308.

[20] S. Odongo, Y.G. Sterckx, B. Stijlemans, D. Pillay, T. Baltz, S. Muyldermans, S. Magez, An anti-proteome nanobody library approach yields a specific immunoassay for Trypanosoma congolense diagnosis targeting glycosomal aldolase, PLoS Negl. Trop. Dis. 10 (2) (2016) e0004420.